Original Paper

Effects of phase separation and devitrification processes in oxide glasses on ESR spectra[1)]

Marianne Nofz

Bundesanstalt für Materialforschung und -prüfung, Berlin (Germany)

Reinhard Stösser and Gudrun Scholz

Chemisches Institut, Humboldt-Universität, Berlin (Germany)

The consequences of phase separation and devitrification processes for the ESR patterns of Fe^{3+} ions and oxygen hole centres in glassy and glassy-crystalline systems are discussed. Analysis of the Fe^{3+} spectra by simulation (including 4th order terms) allows their model-based interpretation for homogeneous, phase-separated and devitrified samples as well. It is even possible to estimate the ratio of Fe^{3+} ions incorporated into the glassy matrix to those localized in the crystalline phase.

An influence of irreversible structural reorganization in glasses on γ-irradiation-induced oxygen hole centres is detectable by studying their saturation behaviour. For the example of a barium silicate glass studied here, pronounced passage effects could be detected at 77 K. In contrast, a devitrified sample of the same composition after γ irradiation yielded the same spectral pattern at low microwave power, but only saturation broadening was to be observed when rising the microwave power.

In an annealed sample of anorthite composition (in mol%: 25CaO, $25Al_2O_3$, $50SiO_2$) progressive crystal growth was detectable using Fe^{3+} ions as probes.

Einfluß von Phasentrennung und Entglasungsprozessen in Oxidgläsern auf ESR-Spektren

In der vorliegenden Arbeit werden Auswirkungen von Entmischungs- und Entglasungsprozessen auf die ESR-Spektren von Fe^{3+}-Ionen und Sauerstoff-Loch-Zentren diskutiert. Die Analyse der Fe^{3+}-Spektren durch Simulation (Einbeziehung von Termen bis zur 4. Ordnung) gestattet deren modellmäßige Interpretation für homogene, entmischte und entglaste Proben. Es ist sogar möglich, den Anteil der Fe^{3+}-Ionen, die in das Glasnetzwerk bzw. die kristalline Phase eingebaut wurden, abzuschätzen.

Ein Einfluß der genannten Prozesse auf strahleninduzierte (γ-Strahlung) Sauerstoff-Loch-Zentren ist durch die Untersuchung des Sättigungsverhaltens nachweisbar. Das hier als Beispiel angegebene Bariumsilicatglas wies bei 77 K ausgeprägte Passageeffekte auf. Eine entglaste γ-bestrahlte Probe dieser Charge zeigte bei kleiner Mikrowellenleistung das gleiche ESR-Signal, jedoch war bei Erhöhung der Mikrowellenleistung nur eine Linienverbreiterung (Ergebnis der Sättigung) nachweisbar.

In einer getemperten Probe mit Anorthit-Zusammensetzung (Stoffmengenanteil in %: 25CaO, $25Al_2O_3$, $50SiO_2$) zeigten die Tieffeldspektren der Fe^{3+}-Ionen ein gerichtetes Kristallwachstum an.

1. Introduction

Irreversible structural reorganizations in glasses like phase separation and devitrification are of scientific and technical interest. They can alter the properties of glasses and glass-ceramics in desired and undesired ways. Unfortunately, the latter case appears rather commonly and there is a need to overcome these processes under industrial aspects by suitable choices of the composition as well as the processing and post-processing parameters. On the other hand, there is a genuine interest in analytical information concerning the nature and extent of the structural processes changing the vitreous state of a material. Commonly, methods like electron microscopy, scattering, optical birefringence [1 to 4] are in use and yield the desired information with the necessary precision. Bearing these facts in mind, it is rather unusual to apply the electron spin resonance (ESR), the local spectroscopic method, in this field, however, some examples [5 to 9] already do exist. At least three reasons justify its application:

a) The ubiquitously present Fe^{3+} ions and the easily generable trapped hole centres can be detected without problems by conventional ESR. The resulting parameters (especially fine and hyperfine structures, line widths and width of parameter distributions) sensitively react even to very small structural changes in the neighbourhood of the paramagnetic centres (pc).

b) The local electric field experienced by the pc's is not only created by the first sphere of the coordinating atoms. It rather represents collected contributions of the second and third shells.

c) The ESR experiment is inseparably connected with an effective magnetic field (e. g. the magnetic induction B_0 of the laboratory magnet which governs the direction of

Received December 6, 1996.

[1)] Presented in German at: 70th Annual Meeting of the German Society of Glass Technology (DGG) on June 5, 1996 in Cottbus (Germany).

Table 1. Compositions (in mol%) of the investigated samples

sample	Rb_2O	Cs_2O	BaO	CaO	Al_2O_3	SiO_2
RbS20	20	–	–	–	–	80
RbS30	30	–	–	–	–	70
CsS10	–	10	–	–	–	90
CsS20	–	20	–	–	–	80
CsS30	–	30	–	–	–	70
BaS30	–	–	30	–	–	70
CAS	–	–	–	25	25	50

quantization). This opens the unique possibility to check even small deviations from the macroscopically isotropic state of a sample by changing its orientation with respect to B_0. In other words, the ESR can be used to detect the locally relevant initial steps of irreversible structural reorganization (like devitrification or phase separation).

Therefore, it is the aim of the present paper to show, how ESR indicates the processes mentioned above if Fe^{3+} ions and trapped holes serve as monitors. Furthermore, examples of the analysis of the complex spectra will be given by spectra simulations.

2. Experimental

The glass samples of the compositions given in table 1 were prepared by using the respective alkali and alkaline earth carbonates as well as $Al(OH)_3$, and SiO_2, and producing a melt in covered platinum crucibles at 1550 °C. The homogeneous melt was poured into steel moulds and then cooled down either in a desiccator (alkali-containing ones) or in a furnace (BaS30, CAS) held at 50 K above the estimated transformation temperature for 1 h and then cooled down to room temperature. Further different temperature treatments were performed on selected samples and will be described in the text below.

For γ irradiations (^{60}Co) of the samples at room temperature an averaged dose rate of approximately 1 Mrad was applied for 1 h.

X-band ESR spectra were recorded at 77 K/300 K using an ERS300 spectrometer (Zentrum für Wissenschaftlichen Gerätebau, Berlin (Germany)) and the microwave power was varied in the range $200\ nW \leq P_{MW} \leq 100\ mW$.

3. Theoretical background – ESR as a source of information on local and medium-range order

More than fourty years ago the first ESR experiments on glasses were conducted. But even in the last time some progress was made in the interpretation of spectra of transition metal centres, especially Fe^{3+} ions incorporated in the glassy matrix [10]. For general information on the basic principles of ESR one can refer to [11 and 12], and for a review concerning the possibilities of ESR in the field of glass science to [13 and 14].

As generally accepted, a powder of paramagnetically doped (regular) microcrystals as well as a specimen of a corresponding glass as a whole should exhibit no macroscopic anisotropy. On the other hand, the spin-coupling parameters of the ESR appear to be tensors (or in a somewhat simpler sense coupling matrices) which are responsible for the announcement of the local anisotropy of paramagnetic centres in the experiments. This holds even for powders or glasses, too. Therefore, the local properties are accessible by ESR and they represent not only effects of the first coordination sphere of the centres. They also collect effectively the influence of the second and third spheres. Among other things, this means that any deviation from the chaotic distribution of the centre-specific coordination axes must consequently change the values and the distribution of the coupling parameters. Finally, via these parameters and attached distributions the overall patterns of the resulting ESR spectra are changed. In other words, devitrification or phase separation processes of a glass experimentally watched by ESR can only be understood on the basis of the simulation of the corresponding spectra. In principle, this statement holds for any type of spin system, but in this work a restriction to $S' = 1/2$ and $S' = 5/2$ systems will be made.

The basis for such simulations is given by a phenomenological spin Hamiltonian containing the different energetic perturbation contributions as a function of spin operators. For the case discussed here $\boldsymbol{H}_{spin}$ has to represent the following interactions:

$$\boldsymbol{H}_{spin} = \boldsymbol{H}\,(\text{Zeeman- and zero-field-splittings}). \qquad (1)$$

Both terms are in general far away from the isotropic case and especially for Fe^{3+} ions in glasses the second term has to cover contributions up to the fourth order [10, 15 and 16]. Figure 1 schematically depicts the procedure of the calculations of the model spectra, which were compared with the experimental ones. The experimental spectrum of traces of Fe^{3+} ions in silicate glasses is characterized by an asymmetric signal centred at an effective g factor g' of 4.3 which is accompanied by two resonances at $g' = 8.6$ and 2, respectively. The analysis of these signals is the aim of the simulation. It uses a fourth order spin Hamiltonian including the zero field parameters D and E and the quartic fine-structure coupling parameters a and F [11]

$$\boldsymbol{H}_{spin} = \beta_e \boldsymbol{B}\, g\, \boldsymbol{S} + \boldsymbol{S}(D, E, \boldsymbol{a}, \boldsymbol{F})\, \boldsymbol{S} \qquad (2)$$

where β_e = Bohr magneton; $\boldsymbol{B}$ = magnetic induction vector; g = g parameter matrix; $\boldsymbol{S}$ = electron spin angular-momentum vector. For calculating the spectra D = = 9250 MHz and $E = 1/3\ D$ were kept constant and appropriate line shape functions were chosen. For $\boldsymbol{a}$ and $\boldsymbol{F}$ a two-dimensional Gaussian distribution was assumed and the corresponding spectra were computed. Their superimposition with weights given by the probability P (up to 70 single spectra) gave the calculated spectrum, which could reproduce the observed experimental line shape.

Concerning the typical ESR X-band pattern of the Fe^{3+} ions and the trapped holes, respectively, some instructive examples are presented in figures 2a to e. A sym-

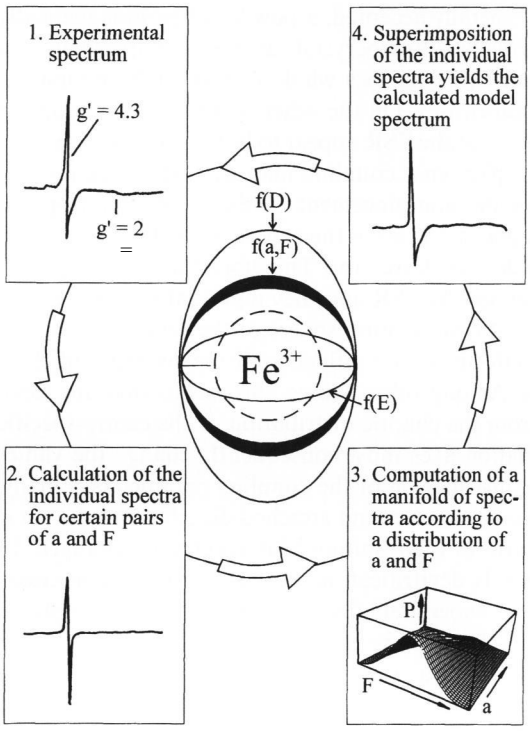

Figure 1. Scheme of the simulation of the ESR spectra of 3 d^5 ions incorporated into amorphous media.

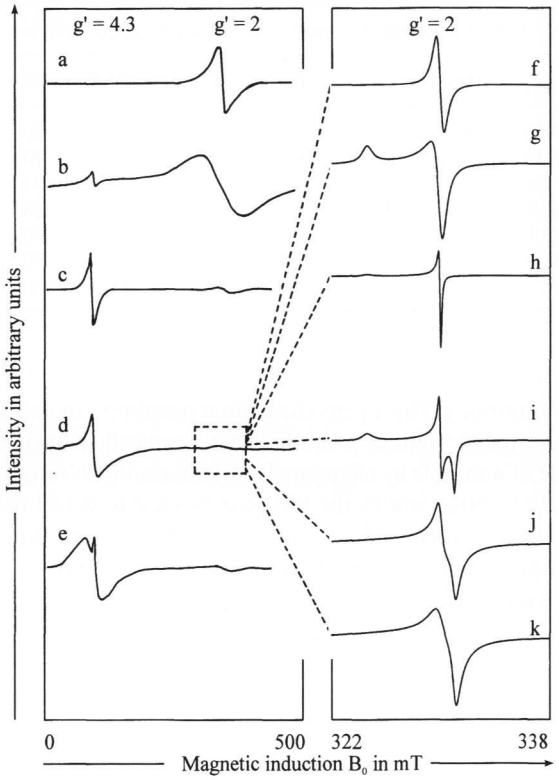

Figures 2a to k. Some general ESR features of Fe^{3+} ions ($S = 5/2$) and trapped holes ($S = 1/2$) observed on powdered crystalline and glassy samples;
a) cubic systems: D, $E = 0$; a, $F \neq 0$;
b) aggregates of $Fe^{3+}-O-Fe^{3+}$, $Fe^{3+}-O-Fe^{2+}$ subunits;
c) orthorhombic systems: D, E, a, $F \neq 0$;
d) typical X-band ESR of Fe^{3+} in oxide glasses;
e) Fe^{3+} in partially devitrified glass;
f) to k) simulated spectra obtained for defects with $S' = 1/2$ using the parameters given in table 2.

metric line at $g' = 2$ is characteristic for a crystalline, cubic system, which is to be described by D, $E = 0$ and a, $F \neq 0$ (figure 2a). If aggregates of $Fe^{3+}-O-Fe^{3+}$ or $Fe^{3+}-O-Fe^{2+}$ subunits appear (figure 2b), then a broad resonance at $g' = 2$ is detectable. The line broadening is the result of magnetic interactions between the neighbouring ferric and ferrous iron ions. Additionally, a resonance at $g' = 4.3$ caused by Fe^{3+} ions in an orthorhombically distorted coordination sphere (figure 2c) can be observed. Figure 2e represents the Fe^{3+} pattern of a partially devitrified glass, caused by superimposed signals of the type shown in figures 2c and d. It follows that a relevant difference between Fe^{3+} ions incorporated into a crystalline system with local orthorhombic symmetry and those incorporated into a glassy matrix results from the distribution of the zero-field-splitting parameters [10].

In glasses bearing a low level of iron ions (e.g., traces of impurities) trapped hole centres can synchronously be used to provide information concerning some relevant aspects of the local structure of a glassy matrix. As figures 2f to k show, the symmetry of the local electric fields surrounding the hole centre is clearly reflected by the habit of the model spectra. Especially, the variation of the line widths (figures 2i to k and table 2) and the distribution of the components of the g tensor [17] are of significant influence on the resulting spectral pattern.

Table 2. g factors and line widths used for simulating the spectra ($S' = 1/2$) shown in figures 2f to k

spetrum	g factor			line width in mT		
	g_1	g_2	g_3	ΔB_1	ΔB_2	ΔB_3
figure f	2.0098	2.0098	2.0098	0.50	0.50	0.50
figure g	2.0440	2.0098	2.0098	0.50	0.50	0.50
figure h	2.0440	2.0098	2.0098	0.50	0.10	0.10
figure i	2.0440	2.0098	2.0034	0.50	0.10	0.15
figure j	2.0440	2.0098	2.0034	5.00	0.30	0.30
figure k	2.0440	2.0098	2.0034	5.00	0.70	0.30

4. Results – Examples for ESR-detected irreversible changes in glasses

As figure 3 mirrors, the ESR spectra of Fe^{3+} ions present as impurities in the rubidium and caesium silicate glasses yield undoubted evidence for significant deviations from the glassy state of the specimens studied. It should be noted that these glasses were investigated without performing any thermal or other post-processing procedure. The splittings of the signals at $g' = 4.3$ (for comparison figure 2d shows the typical low-field Fe^{3+} signal in glasses) undoubtedly and sensitively indicate the coexistence of glassy and partially crystalline regions in the samples. From microscopic and other studies it is known that glasses of such composition tend to segregate and the ESR here gives a microscopic indication of the first steps

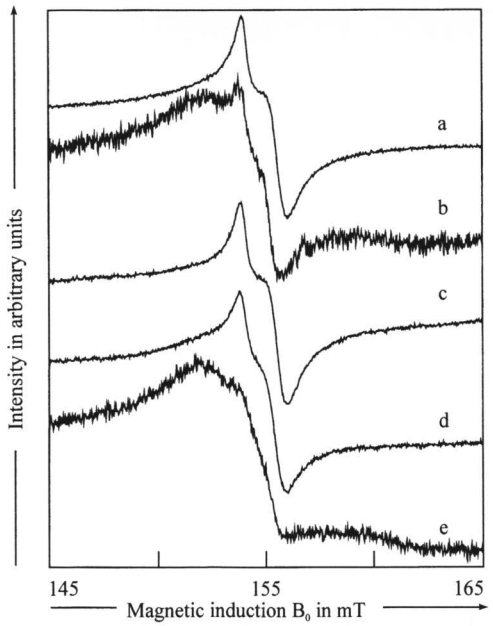

Figures 3a to e. Low-field ESR spectra ($g' \equiv 4.3$; 77 K; $P_{MW} \equiv$ $\equiv$ 20 mW) of alkali silicate glasses; a) RbS20, b) RbS30, c) CsS10, d) CsS20, e) CsS30.

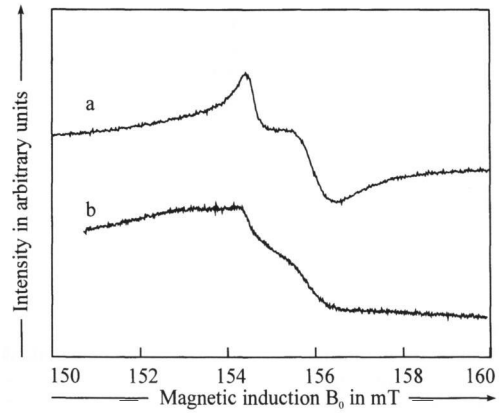

Figures 4a and b. Low-field ESR spectra ($g' \equiv 4.3$; 77 K; $P_{MW} \equiv 20$ mW) of a) the glassy sample BaS30, b) the devitrified product obtained after annealing a specimen of such a glass at 825 °C for 24 h and subsequent γ irradiation.

of such segregation processes. Furthermore, figure 4 represents a typical pattern of thermally induced increasing crystallinity indicated by the ESR of Fe^{3+} ions. The thermal treatment (24 h, 825 °C) here results in the formation of crystallites (50 to 100 µm) observable by light microscopy. Spectral effects showing similar tendencies could be observed and supported by simulations of the spectra of Fe^{3+} ions in layer silicates of different crystallinity [18]. The latter could be proven by X-ray analysis.

As mentioned at the beginning, not only the transition metal ions but also the electronic defects can be used to detect irreversible structural changes in glasses. Figures 5a and b give an impression of the pattern of superimposed signals of HC_1 and HC_2 centres [19] produced by γ ir-

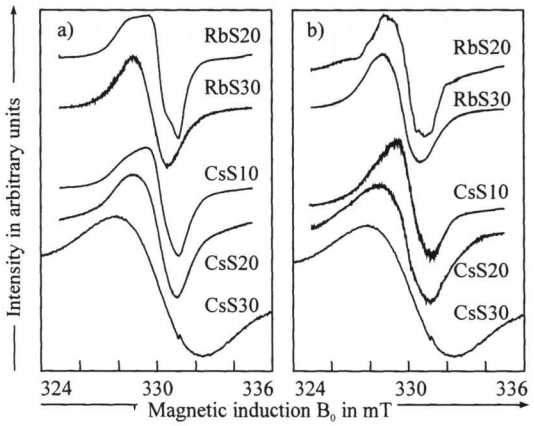

Figures 5a and b. ESR spectra ($g \approx 2$ region, 77 K) of γ-irradiated alkali silicate glasses taken at a) 2 µW, b) 63.2 mW.

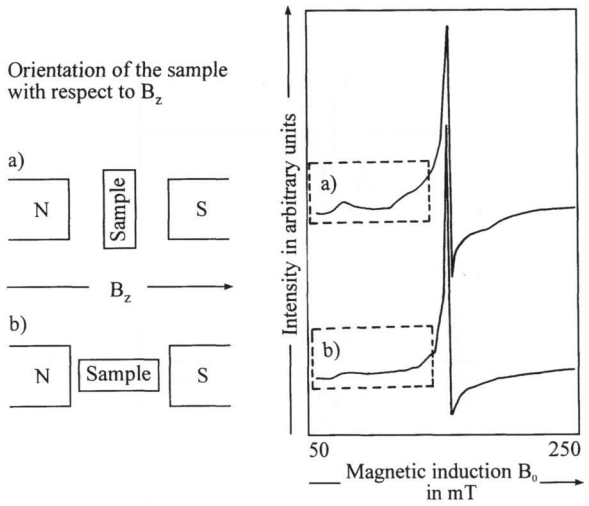

Figures 6a and b. ESR detection of progressive crystal growth in an annealed (1100 °C, 140 h) glass sample of anorthite composition (CAS) using the Fe^{3+} ions as probes; figures a) and b) represent two different orientations of the sample with respect to the direction of the magnetic field.

radiation (figure 5a) and of the response of these species to an enlarged microwave power (figure 5b). The overall pattern of the spectra is governed via the linewidth ΔB_i by the thermal history inducing a partially devitrified state of the matrix. Furthermore, there are only small microwave saturation effects. It is immediately noticeable that especially the caesium-rich glasses exhibit more or less symmetric spectra, which were only slightly affected at the higher power level. Keeping in mind all spectral and temperature-dependent (not shown in this paper) findings one can conclude that here mainly exchange-coupled defects (e.g., interacting trapped holes and electrons $\{h_{tr}^{+} \cdots e_{tr}^{-}\}$) were stabilized. In this case, the internal interactions govern the spectral habit and the changes of the state of the glassy matrix are even better indicated by the individual Fe^{3+} point defects.

The phenomenon of progressive crystal growth in glasses could advantageously be studied by thermal treatment of samples (plates of $(1 \times 10 \times 20)$ mm^3) of the an-

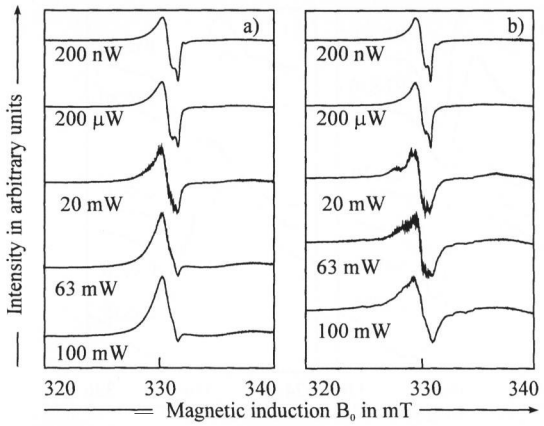

Figures 7a and b. ESR spectra ($g \approx 2$ region, 77 K) of the γ-irradiated glassy sample BaS30 (figure a) and the devitrified specimen obtained after annealing such a glass at 825 °C for 24 h and subsequent γ irradiation (figure b).

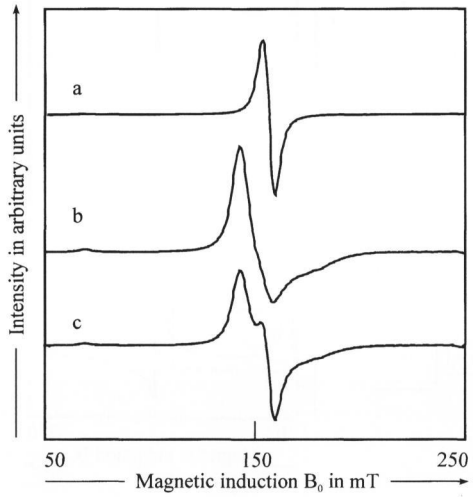

Figures 8a to c. Simulated X-band ESR spectra of a) powder of crystallites doped with Fe^{3+} ions: zero-field-splitting parameters $D = 9250$ Mhz, $E = 1/3\ D$, $\Delta B_i = 2$ mT; b) Fe^{3+}-doped oxide glasses using a two-dimensional Gaussian distribution of the cubic splitting parameters $\boldsymbol{a}$ and $\boldsymbol{F}$; c) superimposition of figures a and b with the ratio 8:1.

orthite composition (in mol%: 25CaO, $25Al_2O_3$, $50SiO_2$). Here not only a change of the spectral pattern caused by the low-field Fe^{3+} fine structure was observed (figures 6a and b). More interestingly, measuring of different orientations of the plates with respect to the direction of the magnetic field (figures 6a and b) even reveals a macroscopic anisotropy of the thermally treated specimens. This anisotropy, caused by progressive crystal growth inside the glassy plates, demonstrates a unique opportunity to apply the ESR method in the field of material science.

An example of how the transformation of a glassy matrix can be detected by low-temperature ESR of γ-irradiated glasses is given in figures 7a and b. It can be seen that the untreated sample gives an ESR response which announces by its shape saturation and passage (100 kHz effect modulation) effects above a microwave power of 20 mW. After a thermal treatment (24 h, 825 °C) both effects were remarkably reduced and there is a correspond-

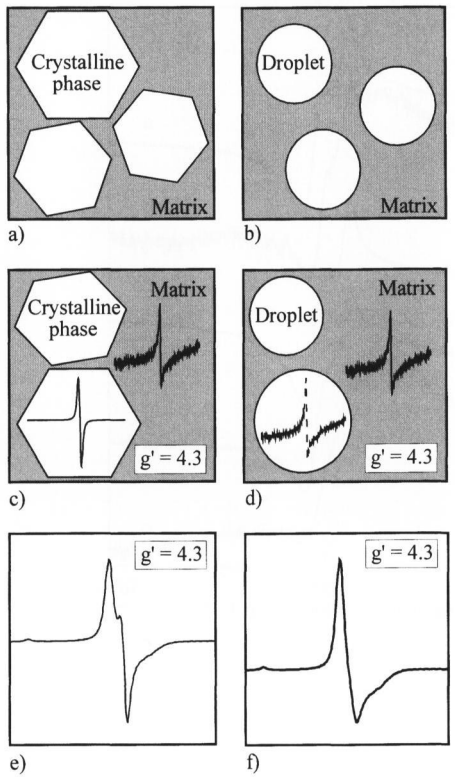

Figures 9a to f. Simplified graphic representation of the correspondence between irreversible processes (phase separation and devitrification) occurring in glasses and the pattern of the ESR response of the Fe^{3+} ions present in the sample;
a) appearence of a crystalline phase in a glassy matrix as a result of devitrification,
b) if phase separation occurs, then, at least, two glassy phases with different chemical compositions coexist in the sample,
c) the patterns of signals caused by Fe^{3+} species being part of the crystalline and glassy phase, respectively, are different concerning the line widths,
d) the habit of Fe^{3+} resonance does not change if the chemical composition of the glasses is altered,
e) result of simulation of the Fe^{3+} spectrum for a devitrified sample obtained by superimposition of the spectra of "two species" (see figure 8c),
f) simulation of the typical "Fe^{3+}-in-glass" pattern, also observed in phase-separated samples.

ence to the result of the segregation process indicated by the Fe^{3+} resonance at $g' \approx 4.3$ which has taken place in the sample. In the course of this process microcrystallites and grain boundaries were formed. The latter possess not only more degrees of freedom, but they are also enriched with iron species enlarging the effectivity of the spin relaxation process.

5. Summary and conclusions

The effects observable by Fe^{3+} ESR were summarized in figures 8a to c using the calculated spectra. Starting with the spectrum of a crystalline system in which the Fe^{3+} ions occupy orthorhombic sites (figure 8a) and superimposing the glass spectrum (figure 8b) as obtained by the procedure shown in figure 1, two kinds of information are accessible by comparison of figure 8c with the experimental results: first, the changes of the spectral pattern (figure

8b) evidence that irreversible structural changes have taken place; second, the weighted superimposition allows to determine the amounts of the crystalline and non-crystalline parts of a sample.

Spectral effects observable for Fe^{3+} species in phase-separated and devitrified samples, respectively, are schematically summarized in figures 9a to f. In an ideal homogeneous glassy network the chemical composition is the same in any region of a sample. A somewhat different situation occurs in the case of devitrification. As indicated in figure 9a, then at least two phases will occur: a glassy matrix and crystallites. They may have either the same or different chemical compositions. But the main difference is related to medium and long-range order. In the crystallite, the structure will be characterized by a more or less distorted lattice periodicity and thus, only a narrow distribution of bond angles and lengths will result. Otherwise, the glassy matrix with its network structure will be characterized by a distinct, broader and specific distribution of these geometric parameters. If no further magnetic interactions occur, then the signals of the crystalline phase are expected to be narrower than those in the glassy matrix (figure 9c). In the result of superimposition of both signals, a pattern of the type shown in figure 9e will be detected.

But, if phase separation occurs, the situation is altered. There will be regions of different chemical compositions, characterized by phase boundaries and usually described as droplets in a matrix (figure 9b). As a consequence of the different chemical compositions of droplet and matrix their network structures could be different. This may be of importance for the formation of different types of trapped holes [19]. But since no pronounced composition dependence for "Fe^{3+}-in-glass" pattern was detected (if the iron concentration was kept constant), the resulting spectral ESR effects do not differ from those of a homogeneous glass. This problem has to be investigated in detail by further studies. It is not clear yet whether the spin dynamics of point defects can indicate phase separation effects.

6. References

[1] Williams, H. P.: Glastechnische Fehler im Behälterglas. In: HVG-Fortbildungskurs 1991: Glastechnische Fabrikationsfehler. 2. Aufl. Frankfurt/M.: HVG, 1992. p. 51–92.

[2] Merker, L.: Schmelzfehler im Flachglas. In: HVG-Fortbildungskurs 1991: Glastechnische Fabrikationsfehler. 2. Aufl. Frankfurt/M.: HVG, 1992. p. 1–50.

[3] Scholze, H.: Glass. Nature, structure, and properties. New York (et al.): Springer, 1991.

[4] Vogel, W.: Glaschemie. Berlin (et al.): Springer, 1992.

[5] Gnappi, G.; Montenero, A.; Giori, D. C. et al.: Crystallization and properties of manganese-sodium-disilicate glasses. Mater. Chem. Phys. **23** (1989) p. 422–432.

[6] Labarbe, P. D.; Lin, J. S.; Weeks, R. A. et al.: Small angle x-ray scattering and electron paramagnetic resonance studies of nucleation and crystallisation in basalt glasses. Phys. Chem. Glasses **29** (1988) no. 2, p. 77-86.

[7] Abdrakhmanov, R. S.; Konoval, E. M.; Shishkin, I. V.: ESR study of the crystallization process in lithium aluminosilicate and calcium magnesium aluminosilicate glasses containing Cr^{III}, Cr^{V}, and V^{IV}. Sov. J. Glass Phys. Chem. **9** (1983) no. 4, p. 281–286.

[8] Bruni, S.; Cariati, F.; Leonelli, C. et al.: Structural modification induced by coloring inorganic oxides in glass-ceramic materials. In: Vincenzi, P. (ed.): Ceramics today – Tomorrow's ceramics. Amsterdam: Elsevier, 1991. p. 677–681.

[9] Andrianasolo, B.; Champagnon, B.; Esnouf, C.: Ultrafine grained glass-ceramics obtained with Cr_2O_3 additions. J. Non-Cryst. Solids **126** (1990) p. 103–110.

[10] Stößer, R.; Scholz, G.; Nofz, M. et al.: On the nature and role of Fe^{3+} ions in oxide and fluoride glasses. Ber. Bunsenges. Phys. Chem. **100** (1996) no. 9, p. 1588–1592.

[11] Weil, J. A.; Bolton, J. R.; Wertz, J. E.: Electron paramagnetic resonance. Elementary theory and practical applications. New York: Wiley, 1994.

[12] Pilbrow, J. R.: Transition ion electron paramagnetic resonance. Oxford: Clarendon Press, 1990.

[13] Griscom, D. L.: Electron spin resonance in glasses. J. Non-Cryst. Solids **40** (1980) p. 211–272.

[14] Stößer, R.; Nofz, M.: ESR spectroscopy on glasses and glassy-crystalline materials. New opportunities for material scientists. Glastech. Ber. Glass Sci. Technol. **67** (1994) no. 6, p. 156–170.

[15] Stößer, R.; Brenneis, R.; Steinfeldt, N. et al.: Electron spin resonance in situ observation of bending stress process in corundum materials and glasses. J. Mater. Sci. **31** (1996) p. 1405–1413.

[16] Scullane, M. I.; White, L. K.; Chasteen, N. D.: An efficient approach to computer simulation of ESR spectra of high-spin Fe(III) in rhombic ligand fields. J. Magn. Resonance **47** (1985) p. 383–397.

[17] Stösser, R.; Nofz, M.; Momand, J.-A. et al.: Correspondence between physical parameters of glasses and defect formation under the influence of high energy irradiation. Glastech. Ber. Glass Sci. Technol. **68 C1** (1995) p. 188–195.

[18] Stößer, R.; Scholz, G.: ESR evidence of order/disorder transitions in solids caused by dehydration- J. Magn. Resonance. (In prep.)

[19] Karakassides, M. A.; Kordas, G.; Mylonas, E. et al.: An electron resonance study of the effect of thermal history on the structure of potassium silicate glasses. Mater. Sci. Eng. **B26** (1994) p. 35–39.

0997P002

Addresses of the authors:

M. Nofz
Bundesanstalt für Materialforschung und -prüfung
Labor V.43 „Glas und Glaskeramik"
Rudower Chaussee 5, D-12489 Berlin

R. Stößer, G. Scholz
Chemisches Institut, Humboldt-Universität
Hessische Straße 1–2, D-10115 Berlin